Available online at www.sciencedirect.com
ScienceDirect

Thermochimica Acta 454 (2007) 26–32

thermochimica acta

www.elsevier.com/locate/tca

Quasi-equilibrated temperature programmed desorption and adsorption: A new method for determination of the isosteric adsorption heat

Wacław Makowski *

Faculty of Chemistry, Jagiellonian University, Ingardena 3, 30-060 Krakow, Poland

Received 4 July 2006; received in revised form 16 November 2006; accepted 17 December 2006
Available online 22 December 2006

Abstract

Temperature programmed desorption and adsorption (TPDA) studied under quasi-equilibrium conditions using typical flow TPD setup equipped with a chromatographic TCD detector has been found a good method of obtaining the equilibrium data characterizing adsorption of *n*-hexane on high silica HZSM-5 and HY zeolites. The equilibrium control of sorption has been confirmed by linearity of the isosters constructed from the TPDA profiles. For HZSM-5 it was corroborated by very good agreement obtained in fitting the experimental data with the model based on the dual site Langmuir (DSL) adsorption function. The values of the adsorption enthalpy and entropy, either determined from the adsorption isosters or as the fitted model parameters, were close to the literature data. Increase of the isosteric adsorption heat of hexane with coverage was observed for both zeolites (72–90 kJ mol^{-1} for HZSM-5 and 46–61 kJ mol^{-1} for HY).

Keywords: Adsorption; Temperature programmed desorption; Isosteric adsorption heat; ZSM-5; *n*-Hexane

1. Introduction

Temperature programmed desorption (TPD) is a well known technique used for characterizing the adsorptive properties of various solids, most often of heterogeneous catalysts [1]. Although many methods for analysis of TPD data were developed, this technique is generally regarded as inaccurate and qualitative only. The main reason of this low opinion is difficulty in separating the kinetic, diffusion and readsorption effects influencing TPD profiles obtained in typical flow setups operating under atmospheric pressure [2]. However, it has been recently reported for several adsorbate/adsorbent system that the thermodesorption rate is in fact controlled by the adsorption–desorption equilibrium. The equilibrium based models have been successfully applied for analysis of TPD profiles of NH_3 desorbing from acidic zeolites [3], CO_2, CH_4 and C_2H_6 from active carbons [4], H_2 from Ni/Al_2O_3 catalysts [5] and *n*-alkanes from various zeolites [6–9], allowing verification of the adsorption functions (isotherms) and/or determination of the adsorption enthalpy.

Thermogravimetric studies on thermodesorption of *n*-alkanes from MFI and FAU zeolites showed that in TPD measurements performed under constant pressure of the adsorptive the adsorption degree is controlled by the adsorption/desorption equilibrium. Methivier and co-workers [6] observed that thermodesorption profiles of C4–C7 *n*-alkanes from silicalite-1 do not depend on the heating rate. Makowski and Majda [7] demonstrated that the TPD profiles of *n*-hexane from ZSM-5 and Y zeolites measured under constant pressure of the adsorptive were identical with the temperature programmed equilibrated desorption (TPED) profiles observed using stepwise temperature programs. In both cases [6,7] the thermodesorption profiles were accurately fitted with functions derived from the Langmuir or dual site Langmuir (DSL) adsorption models and correct values of the adsorption enthalpy and entropy were obtained.

Recently another experimental technique, utilizing a standard TPD system with a chromatographic TCD detector and using He/*n*-alkane mixture as a carrier gas, was successfully applied in studies on thermodesorption of *n*-hexane and *n*-heptane from X, Y and ZSM-5 zeolites [10]. The TPD profiles were similar to the previously reported thermodesorption results. Although they were obtained at changing temperature and concentration of the adsorptive, these TPD profiles could be accurately quantified using a model assuming the equilibrium control of desorption,

---

* Tel.: +48 12 6632245; fax: +48 12 6340515.
E-mail address: makowski@chemia.uj.edu.pl.

0040-6031/$ – see front matter © 2006 Elsevier B.V. All rights reserved.
doi:10.1016/j.tca.2006.12.015

therefore this technique was called quasi-equilibrated temperature programmed desorption (QE-TPD).

The study was focused on further development of the QE-TPD technique, because it seems to have some advantages compared with thermodesorption measurements employing TGA. In the QE-TPD experiments the partial pressure of the adsorptive and the adsorption degree are determined from the measured data, while in the TGA thermodesorption the partial pressure of the adsorptive is usually assumed constant and not monitored. The QE-TPD equipment is cheaper and more flexible than the TGA equipment, it may be easily constructed from the standard elements used in GC instrumentation. It is also less restricted as far as use of various adsorbates is concerned.

The main aim of this study was application of the isosteric approach in analysis of QE-TPD data obtained for *n*-hexane on high silica HZSM-5 and HY zeolites. Analysis of the experimental adsorption isosters (either measured directly or constructed from the isotherms) is a widely used method of determination of the adsorption heat [11]. Since the QE-TPD profiles also represent equilibrium characteristics of adsorption, determination of the isosteric adsorption heat should from these data should be possible as well. Another aim of this work was extending of the QE-TPD technique to temperature programmed adsorption measurements.

Validation of the proposed isosteric method of the QE-TPD data analysis was possible because the studied adsorbate/adsorbent systems are well characterized. Adsorption of *n*-hexane on MFI-type molecular sieves has been extensively studied mainly because of peculiar adsorption isotherms and isobars exhibiting a step at loading of about 50% of maximum sorption capacity [12,13]. This step was attributed to the phase transition of the adsorbed molecules resulting in their ordering and suppressing their mobility. This transition, referred to as the “commensurate freezing”, was predicted by molecular simulations [13] and confirmed by NMR studies [14]. The concept of commensurate freezing is supported by the increase of the absolute values of adsorption entropy and enthalpy with increasing loading [6–8,15–17].

Although the adsorption isotherms of *n*-hexane on Y zeolites may be assigned to type I of the Brunauer classification, they do not fit exactly the profiles derived from the Langmuir adsorption model [8,18], mainly because of the intermolecular interactions of the molecules adsorbed in the supercages of FAU structure. These interactions are reflected by an increase of the adsorption heat with loading [18].

2. Experimental

Commercial zeolites HZSM-5 (Akzo Nobel, Si/Al = 66) and HY (dealuminated, Si/Al = 17, Degussa) were used in this study. Analytical pure *n*-hexane (POCh, Poland) were used as a sorbate. For the TPD measurements the zeolites were pressed into pellets, crushed and sieved. Samples of about 5–10 mg of the sieve fraction 0.35–0.50 mm were used. The zeolites were earlier characterized by the low temperature N_2 adsorption [7] and scanning electron microscopy. The observed isotherms of N_2 adsorption, typical for microporous materials, confirmed presence of micropores of 0.5 nm in diameter for ZSM-5 and 0.7 nm for Y, with very small contribution of meso- and micropores. SEM images revealed that the studied zeolites consisted of small crystallites of about 1–2 μm.

The temperature programmed desorption and adsorption experiments were performed using a homemade TPD setup equipped with a thermal conductivity detector with two independent measuring cells (Valco MicroVolume TCD) connected to the inlet and outlet of a quartz tube (o.d. 6 mm, 15 cm long) containing the sample. The sample tube was placed vertically inside a small coiled heating element that was equipped with a ventilator and controlled by an electronic PID temperature programmer (RE19, Lumel, Poland).

Helium (5.0, Messer) was used as a carrier gas. In the TPD setup there were two independent carrier gas streams controlled by mass flow controllers (Brooks) that could be easily switched between the reactor and its bypass by means of a four port valve. One of the carrier gas lines was equipped with a diffuser (a glass bulb containing the liquid hydrocarbon (HC) with the attached capillary) that was continuously adding a small admixture of the HC vapor to the stream of He. The diffusion rate of the HC into the carrier gas stream was measured gravimetrically in 24 h intervals. It was used for determining the concentration of the HC in the carrier gas as well as for calculating the calibration constant, being the proportional coefficient between the detector signal and the concentration value. Using the diffuser stable concentrations of *n*-hexane in He of about 0.5 vol.% could be obtained even for prolonged periods. All the lines were heated in order to avoid any condensation or adsorption of the HC vapors.

Prior the experiments each sample was activated by heating in a flow of pure He to 450 °C at 10 °C/min and then cooled down. After activation adsorption was performed at room temperature, by switching the flow of He/HC mixture through the reactor until a breakthrough in the TCD signal at the reactor outlet was observed. When the signal stabilized the TPDA experiment was performed by heating the sample with the preadsorbed HC in the flow of He/HC mixture (7.5 cm^3/min) according to a complex temperature program consisting of 5 heating and 5 cooling ramps, with heating rates of 10, 8, 6, 4 and 2 °C/min (see Fig. 1).

3. Results

An example of the TPDA results obtained for HZSM-5/*n*-hexane is presented in Fig. 1. The maxima of the detector signal result from desorption, the minima from adsorption, and the initial increase is caused by the change of the carrier gas (i.e. replacing pure He with He containing 0.51% *n*-hexane). The TPDA results plotted as temperature dependence (Fig. 2) show that positions of the maxima are shifted to higher temperatures with the increasing heating rate, while for the minima an inverse shift is observed.

The experimental TPDA profiles were fitted using a quasi-equilibrium model, assuming temporary adsorption–desorption equilibrium in the perfectly stirred differential reactor. This model was earlier proposed for discussing TPD results [10]. The

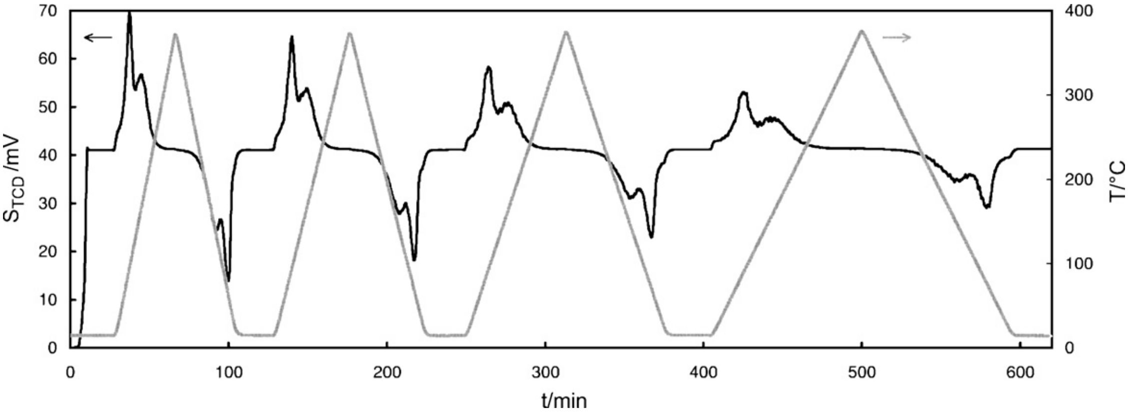

Fig. 1. Sample TPDA results of *n*-hexane on HZSM-5: the temperature program (heating/cooling rates: 10, 8, 6 and 4 °C/min) and the corresponding outlet concentration profile.

model is defined by the Eq. (1) stating the adsorbate balance

$$\frac{d\theta}{dt} = \frac{F}{V_{\mathrm{mol}} a_{\mathrm{m}} p_{\mathrm{t}}}(p_{\mathrm{in}} - p) \tag{1}$$

where F is a flowrate of the carrier gas, V_{mol} a molar volume of gas, p_{t} the total pressure, p_{in} and p the partial pressures of the adsorptive, p_{in} at the sample cell inlet, p inside the sample cell and at the outlet, and temperature T is changing according to the linear temperature program $T = T_0 + \beta t$. Accumulation of the adsorptive in the gas phase is neglected, since it is very small compared with the adsorption capacity of the sample (due to very small volume of the sample cell and low concentration of the adsorptive). The numerical solution of this equation gives evolution of the adsorption value with time. Profile of the partial pressure of the adsorptive in the sample cell may be calculated as

$$p = p_{\mathrm{in}} - \frac{V_{\mathrm{mol}} a_{\mathrm{m}} p_{\mathrm{t}}}{F}\frac{d\theta}{dt} \tag{2}$$

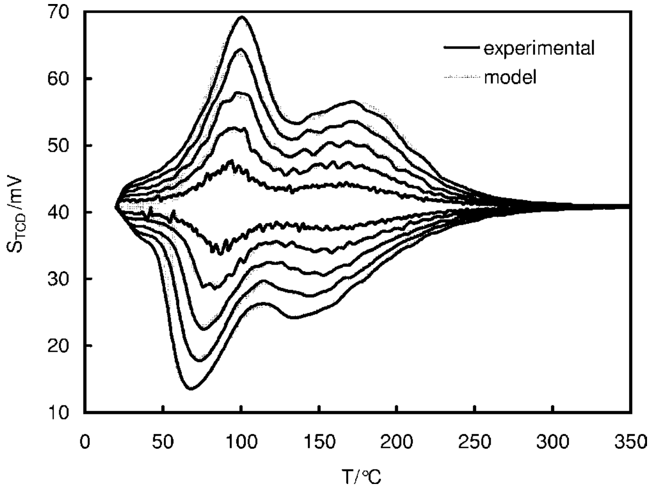

Fig. 2. Temperature dependence of the experimental and model TPDA profiles of *n*-hexane on HZSM-5 (black and gray lines, respectively). The model profiles were obtained by fitting the differential equation defining the TPDA model to the experimental data shown in Fig. 1.

It was assumed that although the partial pressure of the adsorptive in the cell is not constant, it results from a temporary equilibrium with the adsorbate, depending on the adsorption extent and temperature, according to the inverse adsorption function. For the Langmuir adsorption function

$$\theta = \frac{a}{a_{\mathrm{m}}} = \frac{K_{\mathrm{ads}} p}{1 + K_{\mathrm{ads}} p} \tag{3}$$

where θ is a coverage or micropore filling fraction, a the actual, a_{m} the maximum adsorption value, p a partial pressure of the adsorptive and K_{ads} is the adsorption equilibrium constant), the inverse adsorption function is

$$p(T, \theta) = \frac{1}{K_{\mathrm{ads}}}\frac{\theta}{1-\theta} \tag{4}$$

In the case of the dual site Langmuir adsorption function

$$\theta = \frac{a_{\mathrm{m1}}}{a_{\mathrm{m1}} + a_{\mathrm{m2}}}\frac{K_{\mathrm{ads1}} p}{1 + K_{\mathrm{ads1}} p} + \frac{a_{\mathrm{m2}}}{a_{\mathrm{m1}} + a_{\mathrm{m2}}}\frac{K_{\mathrm{ads2}} p}{1 + K_{\mathrm{ads2}} p} \tag{5}$$

the inverse adsorption function is more complex, being the solution of a quadratic equation. For the adsorption equilibrium constants the van't Hoff temperature dependence is assumed

$$K_{\mathrm{ads}} = \exp\left(\frac{\Delta S_{\mathrm{ads}}}{R}\right)\exp\left(-\frac{\Delta H_{\mathrm{ads}}}{RT}\right) \tag{6}$$

The TPD model was fitted to the experimental data using Matlab 6.5. The fitting combined numerical integration of Eq. (1) and optimization of the parameters of the DSL adsorption function (a_{m1}, ΔS_{ads1}, ΔH_{ads1}, a_{m2}, ΔS_{ads2}, ΔH_{ads2}) using Nelder–Mead method. The actual values of the other parameters (F and p_{in}) were taken into these computations. Also the actual temperature profiles were used, because they were not ideally linear and could not be well described by one parameter β. The initial adsorption value θ_0 was set to 0.99, but before starting the temperature ramp the system was allowed to reach the steady state value of θ_0 corresponding to the initial temperature T_0. The low temperature parts of the experimental TPD profiles, clearly deviating from the model profiles, were neglected in the optimization procedure. Because of very long computation time the fitting was performed for only one pair of the experimental TPDA profiles, corresponding to the highest heating and cooling rate. Then the profiles for the other ramps were computed basing on the estimated adsorption parameters.

The results of the fitting are shown in Fig. 2 (gray lines). Apart from a narrow low temperature range (below 60 °C) very good agreement between the model and the experimental TPDA profiles was obtained. The model very well reproduces positions of the maxima and minima for all the heating and cooling rates, although only part of the experimental data was actually used in the optimization. A close-up of one desorption profile (measured at 4 °C/min) is plotted in Fig. 3, along with the corresponding heating rate profile. It should be noticed that the perturbations of the heating rate of about 0.5 °C/min coincide with those in the experimental TPD signal and that similar perturbations appear also in the fitted TPD profile.

Good agreement between the experimental and the model TPDA profiles confirmed the assumption of quasi-equilibrium control of the adsorption, therefore the TPDA data were used for constructing the adsorption and desorption isosters and calculating the isosteric adsorption enthalpy and entropy. Each adsorption and desorption profile was integrated and coverage versus temperature relations were calculated

$$A(T_0, T) = \int_{T_0}^{T} S_{\mathrm{TCD}}\,\mathrm{d}t \tag{7}$$

$$\theta(T) = 1 - \frac{A(T_0, T)}{A(T_0, T_\mathrm{f})} \tag{8}$$

where T_0 is the initial, and T_f is the final temperature of the desorption peak or the adsorption minimum. For a series of θ values (from 0.1 to 0.9, with 0.05 step) the corresponding values of temperature and the detector signal were determined. The signal is proportional to the partial pressure of the adsorptive at the sample cell outlet, since it was compensated to zero for pure He. The isosters constructed for each θ value are shown in Fig. 4 as $\ln S_{\mathrm{TCD}}$ versus $1/T$ plots. It may be noticed that the linearity of the isosters is very good and there are only very small differences in slope and intercept between their adsorption and desorption parts.

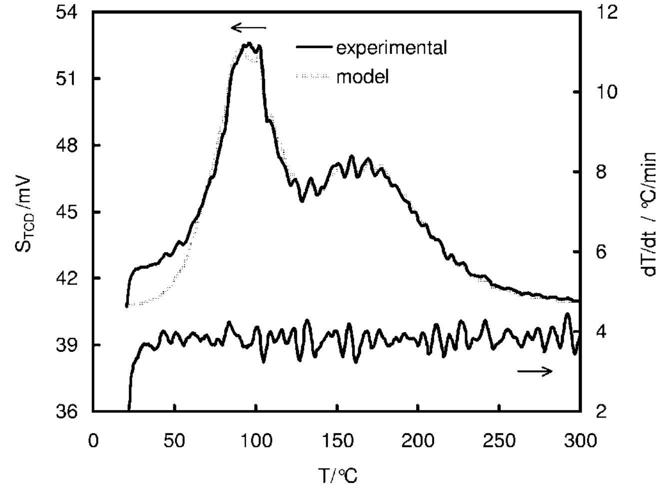

Fig. 3. Influence of the perturbations of the heating rate on the experimental and model TPDA profiles of *n*-hexane on HZSM-5.

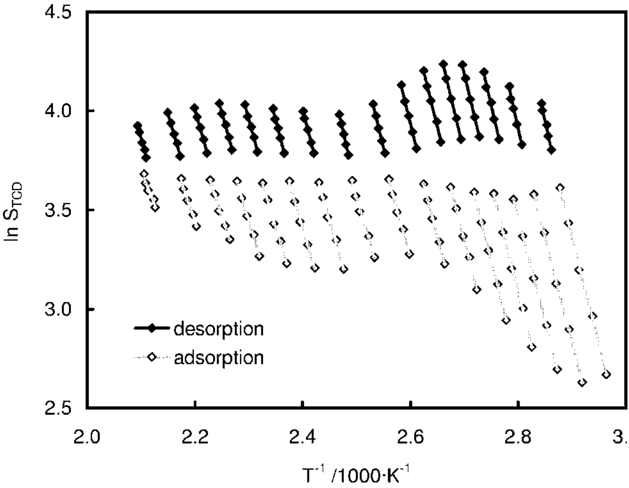

Fig. 4. Isosters of desorption and adsorption of *n*-hexane on HZSM-5 generated from TPDA results shown in Fig. 1.

The isosteric adsorption heat q_{isost} was calculated from the slope of the isosters

$$\ln S_{\mathrm{TCD}} = \mathrm{const} - \frac{q_{\mathrm{isost}}}{RT} \tag{9}$$

Basing on the values of q_{isost} the differential molar entropy of adsorption was determined [15]:

$$\Delta S_{\mathrm{ads}} = R \ln\left(\frac{p^{\mathrm{o}}}{p}\right) - \frac{q_{\mathrm{isost}}}{T} \tag{10}$$

where p^{o} is the standard pressure (1.0135×10^5 Pa). The values of q_{isost} and ΔS_{ads} obtained from the experimental desorption and adsorption isosters for different θ values are plotted in Fig. 5, along with the corresponding values obtained using the fitted TPDA profile as well as the literature data reported by Rees et al. [15,16]. There is a good agreement between the literature data and the values of q_{isost} and $(-\Delta S_{\mathrm{ads}})$ calculated from the experimental adsorption desorption isosters, while those determined from the desorption isosters are noticeably higher. However, the accuracy of the latter values is lower, as indicated by the error bars (which represent the errors resulting from uncertainty of the linear regression parameters). Very good agreement between the values of the isosteric adsorption heat and adsorption entropy calculated for the adsorption isosters obtained from the experimental and fitted TPDA profiles validates the model used for fitting. More literature data to be compared with the thermodynamic parameters characterizing adsorption of *n*-hexane on HZSM-5 determined from the TPDA results are listed in Table 1. It should be pointed out that the TPDA-based parameters reproduce well simultaneous increase of the adsorption heat and the entropy change for adsorption $(-\Delta S_{\mathrm{ads}})$ with the coverage, with two plateau regions at 25 and 75% of the maximum sorption capacity and an inflexion point at 50%. These characteristic points are clearly visible in the trends determined from the sim-

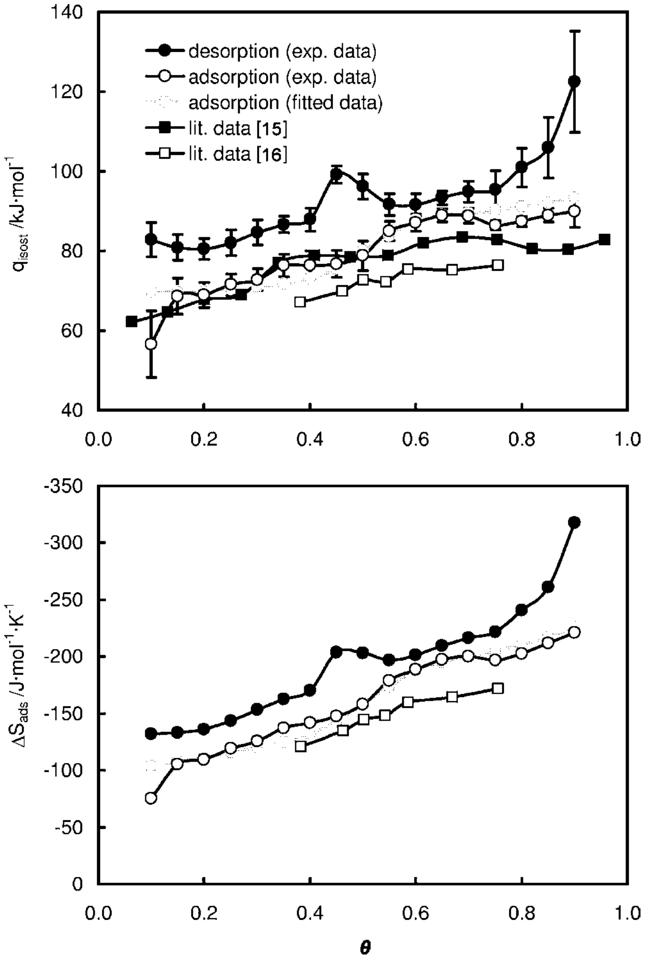

Fig. 5. Comparison of coverage dependences of the isosteric adsorption heat and the adsorption entropy of *n*-hexane on HZSM-5 (determined from the experimental or fitted TPDA profiles) with the literature data [15,16].

ulated TPDA profiles. Such dependences were often quoted as an explanation of the complex adsorption and desorption patterns of *n*-hexane on MFI molecular sieves (“the commensurate freezing effect”) [15,17].

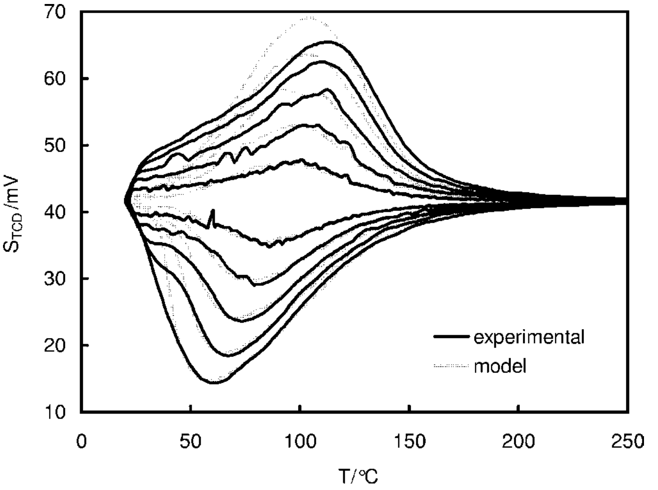

Fig. 6. Experimental and model TPDA profiles of *n*-hexane on HZSM-5 (black and gray lines, respectively).

In Fig. 6 the experimental TPDA profiles of *n*-hexane on HY zeolites are depicted, together with the results of fitting. Because there was only one desorption/adsorption peak in the TPDA profiles, the fitted model was in this case based on single Langmuir adsorption function. However, the intensities of the desorption peaks are considerably lower than those of the adsorption peak. Such TPDA profiles may not be fitted using single Langmuir adsorption function, therefore only the adsorption part of the experimental data was taken into account during fitting. The quality of the fit is quite low—it reproduces well the adsorption parts, but the fitted desorption maxima are less intensive and shifted to higher temperatures than the experimental ones. Despite these discrepancies the isosters constructed from the TPDA data (Fig. 7) are fairly linear and their adsorption and desorption parts do not differ considerably in slope and intercept (apart from those determined for very low coverage). These results confirm the equilibrium control of TPDA experiments also for *n*-hexane/HY systems.

Table 1
Values of the adsorption enthalpy and entropy determined from the TPDA profiles: (A) by fitting the model based on the DSL or the Langmuir adsorption function and (B) from the adsorption isosters, compared with the literature data

Zeolite	$-\Delta H_{ads}$ [kJ mol^{-1}]			$-\Delta S_{ads}$ [J mol^{-1} K^{-1}]		
	A	B (q_{isost})	Literature data	A	B	Literature data
HZSM-5^{I}	93	86 ($\theta = 0.75$)	102[a], 88[b], 78[c], 76[d], 73[e]	212	196 ($\theta = 0.75$)	237[a], 204[b], 188[c], 172[d], 196[e]
HZSM-5^{II}	70	72 ($\theta = 0.25$)	66[a], 62[b], 72[c], 67[d], 67[e], 70[f], 68–77[g]	117	119 ($\theta = 0.25$)	107[a], 103[b], 122[c], 121[d], 148[e]
HY	64	51 ($\theta = 0.5$)	63[a], 58[b], 48–50[h], 47–65[i]	131	98 ($\theta = 0.5$)	124[a], 114[b]

^{I,II}Peak positions (the literature data correspond to high and low loadings, respectively).

[a] Calculated from the equilibrated TPD data for the same zeolites [10] (calculations based on dual site Langmuir adsorption model).

[b] Calculated from the equilibrated thermodesorption data measured gravimetrically for the same zeolites [8] (calculations based on dual site Langmuir adsorption model).

[c] Calculated from the equilibrated thermodesorption data for silicalite-1 (Si/Al = 380) [6] (calculations based on dual site Langmuir adsorption model).

[d] Isosteric values (for loadings 2.8–5.5 molecules per unit cell on silicalite-1) [13].

[e] Calculated from the adsorption isotherms for silicalite-1 (Si/Al > 1300) [15] (calculations based on dual site Langmuir adsorption model).

[f] From molecular simulations [19].

[g] Determined for HZSM-5 (Si/Al = 12–250) from the IGC data [20].

[h] From molecular simulations [21].

[i] Calorimetric data (for loadings 0–1.53 mmol/g on high silica FAU (Si/Al = 300) [18].

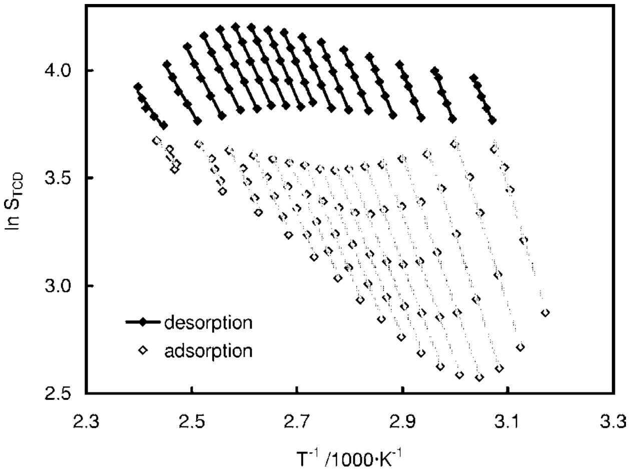

Fig. 7. Isosters of desorption and adsorption of *n*-hexane on HY generated from TPDA results shown in Fig. 6.

Plots of the isosteric adsorption heat and adsorption entropy versus coverage are presented in Fig. 8, along with the coverage dependence of the adsorption heat determined calorimetrically for high silica HY [18]. The values of $q_{\rm isost}$ calculated from the experimental isosters are close to the literature data (see Table 1) and they also increase with coverage. The parameters determined from the fitted desorption profiles are noticeably higher and are practically constant. Such independence might be expected, since the Langmuir adsorption model used for fitting implies equivalence of the adsorption sites. This indicates that such a function cannot adequately describe adsorption of *n*-hexane in HY zeolites. Another type of model functions must be used, taking into account the heterogeneity of the adsorption sites revealed by the coverage dependences of the isosteric adsorption heat and adsorption entropy. These dependences should be attributed to the intermolecular interactions of the adsorbed molecules located in the supercages of the FAU framework.

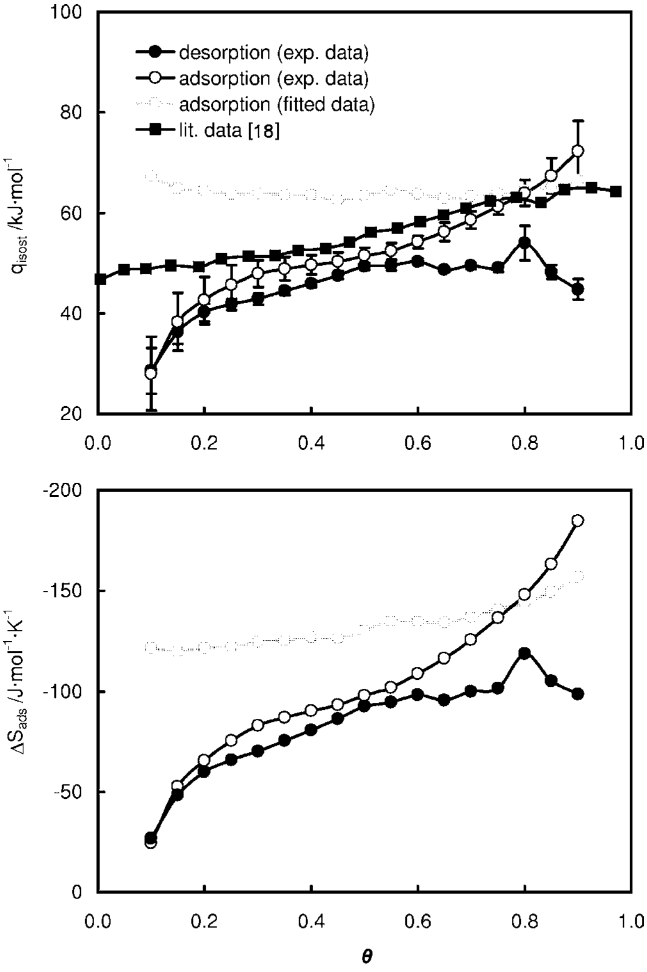

Fig. 8. Comparison of coverage dependences of the isosteric adsorption heat and the adsorption entropy of *n*-hexane on HY (determined from the experimental or fitted TPDA profiles) with the literature data [18].

4. Discussion

All the presented results are consistent with previously reported findings concerning adsorption of *n*-hexane on zeolites. The equilibrium control of adsorption extent in the TPDA experiments was confirmed not only by linearity of the isosters constructed from the TPDA profiles, but also by good agreement of the adsorption enthalpy and entropy values computed from the isosters with the literature data, determined using different experimental techniques (cf. Table 1). For HZSM-5 it was also corroborated by very good fitting of the experimental data with the quasi-equilibrium model based on the dual site Langmuir adsorption function.

Despite the fact that the studied zeolites were in H-exchanged form, neither catalytic cracking of *n*-hexane no coke formation could be detected during TPDA measurements. No substantial differences in the equilibrated thermodesorption profiles of *n*-hexane could be observed in earlier studies for Na- and H-exchanged forms of the same zeolites [7]. Much lower gas phase concentration of *n*-hexane during TPDA experiments (ca. 0.5 mol%) than in the previous TPED experiments (6 mol%) makes any catalytic reaction even less possible. Absence of any deterioration of the zeolites samples in the TPDA experiments was also confirmed by very good reproducibility of the results obtained in consecutive experiments.

Intra-crystalline diffusion may influence the rate of thermodesorption. However, diffusion of *n*-alkanes in zeolites is quite fast [22]. For *n*-hexane/MFI the equilibrium control of thermodesorption was confirmed in gravimetric measurements even at heating rates as high as 5 °C/min [6,7]. Fitting the equilibrium model to the TPDA data gives reasonable values of the adsorption heat and adsorption entropy, close to those obtained by fitting similar adsorption function to the equilibrium data [15]. Diffusion limitations should result in shifting the desorption maxima to higher temperatures and the minima to lower temperatures. These shifts should increase with the heating rate. Therefore, the desorption and adsorption parts of an isoster constructed from diffusion-affected TPDA data should not form one straight line. However, the linearity of the overall isosters constructed from the TPDA data is quite good (apart from those obtained for the highest and the lowest adsorption values), indicating absence of any considerable diffusion limitations.

5. Conclusions

It has been demonstrated that the temperature programmed desorption and adsorption (TPDA), measured under quasi-equilibrium conditions in a flow experimental system equipped with a TCD destector, is a good method of studying adsorption equilibria, allowing determination of the isosteric adsorption heat and adsorption entropy in a wide range of coverage. It was successfully applied for characterizing two *n*-hexane/zeolites systems, but is may be easily extended to any other adsorbate/adsorbent system, provided that the equilibrium control of sorption is maintained.

This novel experimental technique has a number of advantages, among which the most important seems the method of data interpretation free from any assumptions about adsorption models or functions. The only important assumption concerning equilibrium control of desorption may be verified by testing linearity of the isosters determined from the experimental TPDA profiles. Other advantages of this technique are simple, flexible and relatively inexpensive equipment, small amounts of the adsorbent samples needed (ca. 10 mg) and the measurements shorter than those performed using alternative experimental techniques.

References

[1] R.J. Cvetanovic, Y. Amenomiya, Adv. Catal. 17 (1967) 103.
[2] R.J. Gorte, Catal. Today 28 (1996) 405.
[3] T. Masuda, Y. Fujikata, S.R. Mukai, K. Hashimoto, Appl. Catal. A 165 (1997) 57.
[4] J.M. Mugge, Ph.D. Thesis, University of Twente, 2000.
[5] J.M. Kanervo, K.M. Reinikainen, A.O.I. Krause, Appl. Catal. A 258 (2004) 135.
[6] B. Millot, A. Methivier, H. Jobic, J. Phys. Chem. 102 (1998) 3210.
[7] W. Makowski, D. Majda, Thermochim. Acta 412 (2004) 131.
[8] W. Makowski, D. Majda, Appl. Surf. Sci. 252 (2005) 707.
[9] D. Majda, W. Makowski, Stud. Surf. Sci. Catal. 158 (2005) 1161.
[10] W. Makowski, D. Majda, J. Porous Mater. 2006, doi:10.1007/s10934-006-9004-3.
[11] S. Sircar, D.V. Cao, Chem. Eng. Technol. 25 (2002) 10.
[12] R.E. Richards, L.V.C. Rees, Langmuir 3 (1987) 335.
[13] B. Smit, T.L.M. Maesen, Nature 374 (1995) 42.
[14] G.G. Pimenov, O.A. Opanasyuk, V.D. Skirda, J. Kärger, Colloid J. 65 (2003) 60.
[15] Y. Yang, L.V.C. Rees, Microporous Mater. 12 (1997) 117.
[16] L.V.C. Rees, D. Shen, in: H. Van Bekkum, E.M. Flanigen, P.A. Jacobs, J.C. Jansen (Eds.), Introduction to Zeolite Science and Practice, Elsevier Science, Amsterdam, 2001, pp. 579–631.
[17] W. Zhu, F. Kapteijn, B. van der Linden, J.A. Moulijn, Phys. Chem. Chem. Phys. 3 (2001) 1755.
[18] F. Eder, J.A. Lercher, Zeolites 18 (1997) 75.
[19] E. García-Pérez, I.M. Torrens, S. Lago, R. Krishna, B. Smit, S. Calero, Stud. Surf. Sci. Catal. 158 (2005) 1097.
[20] I.C. Arik, J.F. Denayer, G.V. Baron, Microporous Mesoporous Mater. 60 (2003) 111.
[21] S. Calero, D. Dubbeldam, R. Krishna, B. Smit, T.J.H. Vlugt, J.F.M. Denayer, J.A. Martens, T.L.M. Maesen, J. Am. Chem. Soc. 126 (2004) 11377.
[22] A.O. Koriabkina, A.M. de Jong, E.J.M. Hensen, R.A. van Santen, Microporous Mesoporous Mater. 77 (2005) 119.